

# Efficient and Robust Thermoelectric Power Generation Device Using Hot-Pressed Metal Contacts on Nanostructured Half-Heusler Alloys

GIRI JOSHI<sup>1,2</sup> and BED POUDEL<sup>1</sup>

1.—Evident Thermoelectrics, Troy, NY 12180, USA. 2.—e-mail: sushil2035@outlook.com

We report an efficient thermoelectric device with power density of 8.9 W/cm<sup>2</sup> and efficiency of 8.9% at 678°C temperature difference using hot-pressed titanium metal contact layers on nanostructured half-Heusler materials. The high power density and efficiency are due to the efficient nanostructured materials and very low contact resistance of  $\sim 1 \mu\Omega \text{ cm}^2$  between the titanium layer and half-Heusler material. Moreover, the bonding strength between the titanium and half-Heusler is more than 50 MPa, significantly higher compared with conventional contact metallization methods. The low contact resistance and high bonding strength are due to thin-layer diffusion of titanium ( $< 100 \mu\text{m}$ ) into the half-Heusler at high temperature ( $> 600^\circ\text{C}$ ). The low contact resistance and high bonding strength result in a stable and efficient power generation device with great potential for use in recovery of waste heat, e.g., in automotive and industrial applications.

**Key words:** Thermoelectric devices, metallization, half-Heuslers, nanostructuring

## INTRODUCTION

Thermoelectric generators (TEGs), which convert heat into electricity, are now being considered as an alternative and reliable option for waste heat recovery and solar energy harvesting.<sup>1,2</sup> The maximum efficiency ( $\eta_{\text{max}}$ ) of such energy conversion is defined by the operating temperature, namely the temperature difference ( $\Delta T$ ) between the hot ( $T_{\text{h}}$ ) and cold side ( $T_{\text{c}}$ ), and the material thermoelectric figure of merit  $ZT = (\alpha^2 \sigma T) / \kappa$  as shown in Eq. 1.<sup>3</sup>

$$\eta_{\text{max}} = \frac{\Delta T}{T_{\text{h}}} \left[ \frac{\sqrt{1 + ZT_{\text{ave}}} - 1}{\sqrt{1 + ZT_{\text{ave}}} + T_{\text{c}}/T_{\text{h}}} \right], \quad (1)$$

where  $\alpha$  is the Seebeck coefficient,  $\sigma$  is the electrical conductivity,  $\kappa$  is the thermal conductivity,  $T$  is the absolute temperature, and  $ZT_{\text{ave}}$  is the average  $ZT$  value across  $\Delta T$ . However, the efficiency of TEG devices is lower than predicted by Eq. 1 due to various parasitic losses introduced during device

fabrication, e.g., due to electrical and thermal contact resistances between electrodes and TE materials.<sup>4,5</sup> A current challenge is to study such parasitic losses and reduce them as much as possible to maximize the power conversion efficiency. Over the past decade, significant progress has been made in improving  $ZT$  values of thermoelectric (TE) materials such as bismuth telluride (BiTe)-based alloys, lead tellurides, skutterudites, half-Heuslers, silicides, clathrates, and tetrahydrides with peak TE figure of merit above 1.0 in different temperature regimes,<sup>6–18</sup> but very limited research work has been done on device fabrication to provide strong, stable, and good electrical and thermal contacts on TE materials.<sup>19–22</sup> We report herein a pathway to achieve very low contact resistance ( $\sim 1 \mu\Omega \text{ cm}^2$ ) by using a simple hot-pressed metallization technique to fabricate TE legs of nanostructured half-Heusler, using titanium (Ti) as metal layer. The power density and efficiency of such devices were measured as  $\sim 8.9 \text{ W/cm}^2$  and 8.9%, respectively, at  $\Delta T = 678^\circ\text{C}$ . To the best of our knowledge, this is the highest power density

(Received December 1, 2015; accepted May 21, 2016; published online June 9, 2016)

achieved with practical TE devices using bulk thermoelectric materials. Moreover, the bonding strength of these devices is higher than 50 MPa, making them stable for use in high-temperature ( $>500^{\circ}\text{C}$ ) applications. The nanostructured half-Heusler material is chosen over other available materials due to its competitive material performance, good thermal stability,<sup>11–14</sup> excellent mechanical properties,<sup>23</sup> and TEG manufacturing feasibility,<sup>22,24</sup> since these are the most essential factors for use in waste heat recovery, e.g., in automotive and industrial applications, in terms of cost-effective device performance.

## EXPERIMENTAL PROCEDURES

Nanostructured *p*- and *n*-type half-Heusler disks, composed of  $\text{Hf}_{0.5}\text{Zr}_{0.5}\text{CoSb}_{0.8}\text{Sn}_{0.2}$ <sup>11</sup> and  $\text{Hf}_{0.75}\text{Zr}_{0.25}\text{NiSn}_{0.99}\text{Sb}_{0.01}$ ,<sup>13</sup> respectively, with diameter of 0.5 inches were prepared by a cost-effective melting–ball milling–hot pressing route.<sup>7</sup> The hot-pressed disks together with titanium (Ti) foils of  $250\ \mu\text{m}$  on top and bottom were inserted inside a graphite die and hot pressed at  $600^{\circ}\text{C}$  to  $800^{\circ}\text{C}$  to form a strong bond between the half-Heusler and Ti electrodes. The nanostructured disks with Ti electrodes were then cut into  $2.5\ \text{mm} \times 2.5\ \text{mm} \times 2\ \text{mm}$  legs for both *p*- and *n*-type materials to fabricate a TE device with *p*- and *n*-legs connected electrically in series and thermally in parallel. The *p*- and *n*-legs were joined by a metal (copper) interconnect, and a series of such devices was

placed between a heat source ( $T_h$ ) and heat sink ( $T_c$ ), as shown in Fig. 1.

The quality of the hot-pressed Ti layer was analyzed by scanning electron microscopy (SEM) and energy-dispersive spectroscopy (EDS) on the basis of diffusion and bonding formation between Ti and half-Heusler. Furthermore, the contact resistance between the Ti layer and half-Heusler was measured using a custom-built benchtop apparatus based on the scanning probe method (Fig. 2), whereas the bonding strength was measured using commercial equipment (Instron, model 5942). These parameters significantly affect the performance of the final TE device. The electrical power output and efficiency of the TE device were measured using a custom-designed power measurement kit consisting of a “Q-meter” setup (Fig. 3) in vacuum environment. The accuracy of the power measurement kit has been calculated to be around 5% using the standard errors of all instrument components. The standard error for each component was calculated from hundreds of experimental data at similar conditions.

## RESULTS AND DISCUSSION

This paper presents the results for hot-pressed metal (Ti) layer on half-Heusler materials. Figure 4a shows a SEM image of the interface between the Ti layer and half-Heusler, indicating no significant diffusion of Ti on half-Heusler. EDS elemental scans further confirmed that the diffusion layer was no more than  $100\ \mu\text{m}$  (Fig. 4b and c). This amount of diffusion will not affect the material properties but rather helps to create stable and strong bonding and acts as a barrier layer to stop further diffusion of Ti. This diffusion could be due to high-temperature operation at  $600^{\circ}\text{C}$  to  $800^{\circ}\text{C}$ . Furthermore, the SEM image of a TE leg (inset of Fig. 4b) shows that the material consists of nanograins with size less than a micron.

Figure 5 presents the resistance scan across the *n*- (a) and *n*-type (b) legs with Ti hot-pressed metal layer. Figure 5 clearly shows that the electrical contact resistance across the interface of the half-Heusler leg and Ti layer is very low and stable for heat treatment of  $600^{\circ}\text{C}$ . The measured contact resistance for both types of materials is around  $1\ \mu\Omega\ \text{cm}^2$ , exceptionally low compared with conven-

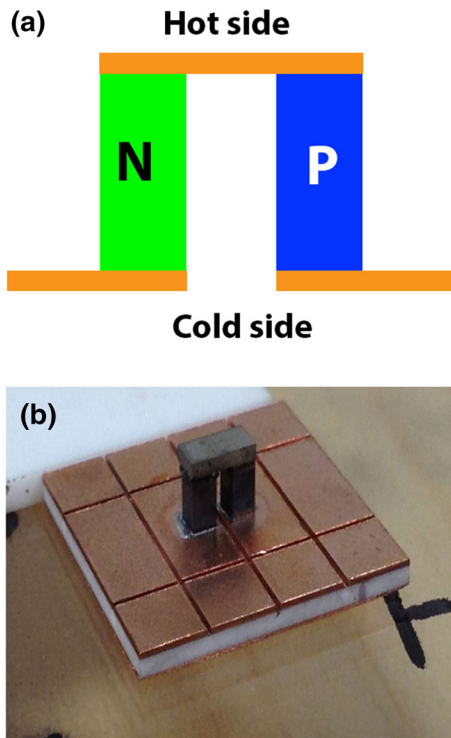


Fig. 1. Thermoelectric device (a) sketch, and (b) fabricated using one *p*- and one *n*-type leg.

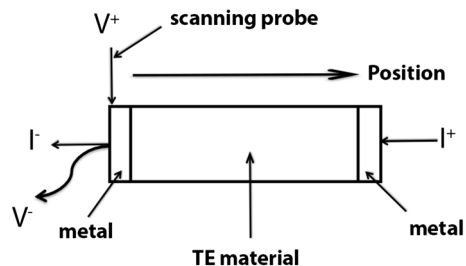


Fig. 2. Sketch of scanning probe method.

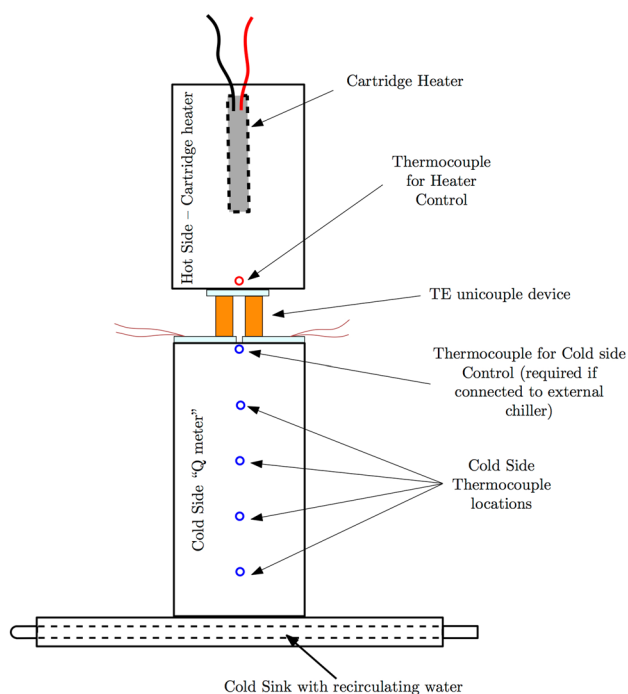


Fig. 3. Q-meter setup to measure TE power, internal resistance, and efficiency.

tional metallization techniques.<sup>5</sup> We also measured very high bonding strength between the half-Heusler and Ti of around 50 MPa, significantly higher compared with traditional metallization techniques ( $\sim 10$  MPa) such as vacuum deposition, thermal spray, etc. Such high bonding strength could result in a stable TE device during long-term operation. The low contact resistance and high bonding strength could be due to strong bonding between half-Heusler atoms and Ti atoms at the diffused interfaces during high-temperature hot pressing ( $600^{\circ}\text{C}$  to  $800^{\circ}\text{C}$ ), being essential factors for efficient TE devices.

Power density, efficiency, and module life are the most important factors in the development of cost-effective practical TE generators; For example, in typical BiTe-based modules, the power density is about  $0.5 \text{ W/cm}^2$ ,<sup>25</sup> making such modules bulky with materials accounting for a significant portion of module cost. By making thinner slices of TE legs, the power density can be improved for every material, in theory. However, thinner legs cause high thermal stress and shorten module life if the contact layer or TE material itself is weak. Since the half-Heusler material strength and contact metallization bonding strength are both exceptionally

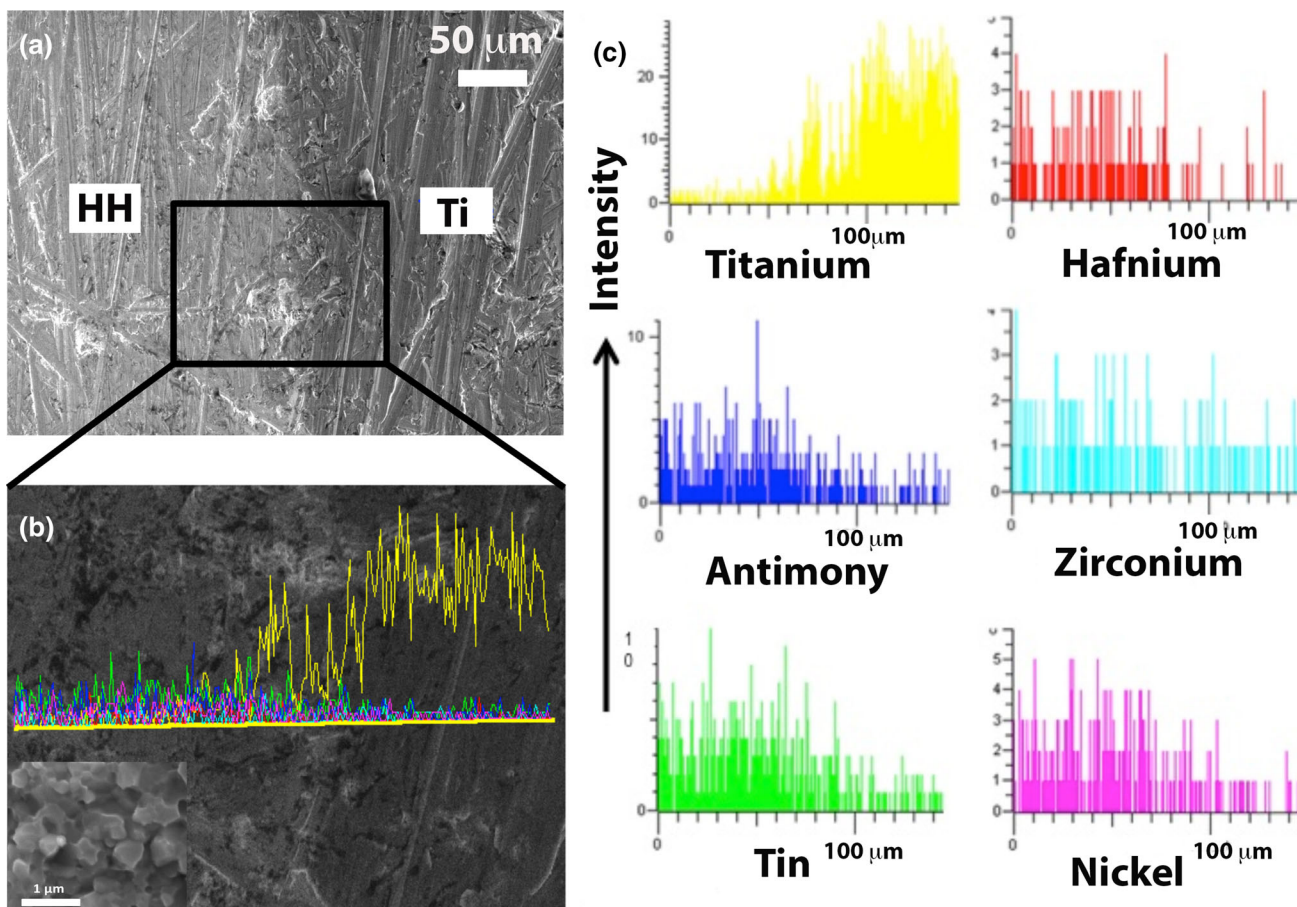


Fig. 4. SEM image (a) and elemental scans (b, c) across the interface of half-Heusler (HH) and titanium (Ti) layer.

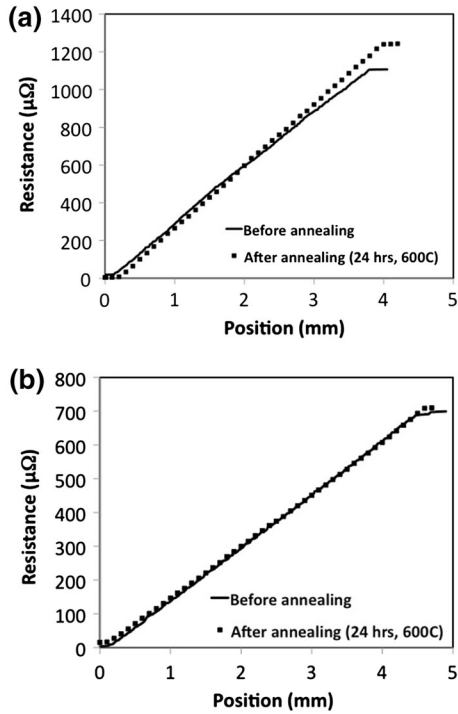


Fig. 5. Resistance scans of  $p$ -type (a) and  $n$ -type (b) HH leg with hot-pressed Ti layer.

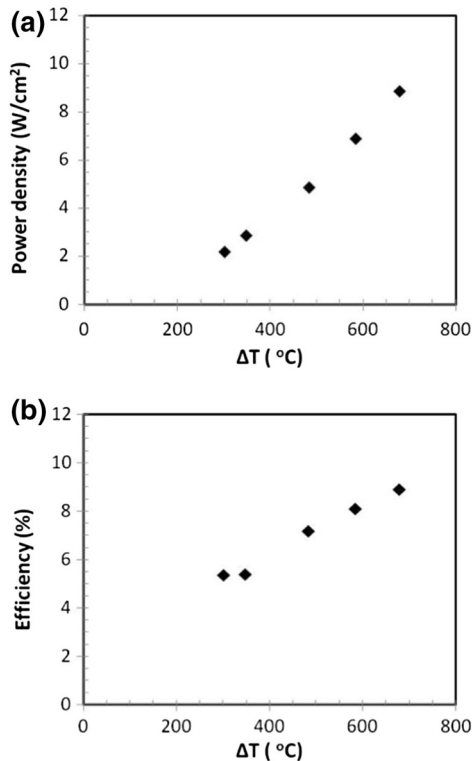


Fig. 6. Power density (a) and efficiency (b) of a HH device using one  $p$ - and one  $n$ -type TE leg of size  $2.5 \text{ mm} \times 2.5 \text{ mm} \times 2 \text{ mm}$ .

high, it is possible to achieve high power density and long module life at the same time. This makes half-Heusler material very attractive for high-temperature power generation applications.

Figure 6 presents the electrical power density (a) and efficiency (b) of a TE device made using nanostructured half-Heusler with hot-pressed Ti contact metal layer for different values of  $\Delta T$  ( $=T_h - T_c$ ). The power density was calculated using the active area of TE legs. Figure 6 clearly shows that the power density and efficiency both increase with increase in  $\Delta T$ , as predicted from Eq. 1. A maximum power density of about  $8.9 \text{ W/cm}^2$  and efficiency of 8.9% were measured from the TE device for  $\Delta T = 678^\circ\text{C}$ . The high power and efficiency of these devices are mainly due to the high-performance nanostructured materials, and the very low contact resistance and strong hot-pressed contact layers. Such high-power, efficient devices have great potential for use in power generation TE devices for recovery of automotive and industrial waste heat.

## CONCLUSIONS

An efficient power generation TE device was fabricated with high power density of about  $8.9 \text{ W/cm}^2$  and efficiency of 8.9% for  $\Delta T = 678^\circ\text{C}$  using nanostructured half-Heusler materials with hot-pressed Ti metallization. Very low contact resistance of  $\sim 1 \mu\Omega \text{ cm}^2$  and high bonding strength of  $\sim 50 \text{ MPa}$  were measured between the hot-pressed Ti layer and nanostructured half-Heusler materials. These efficient TE devices, with strong and stable metallization, have great potential for use in automotive and industrial waste heat recovery applications.

## ACKNOWLEDGEMENT

We would like to thank Prof. Zhifeng Ren, Dr. Chris Caylor, Dr. Jonathan D'Angelo, Dr. Ashwin Rao, and Tej Pantha for their valuable contributions to the work.

## REFERENCES

1. T. Kajikawa, in *CRC Handbook of Thermoelectrics*, ed. D.M. Rowe (Boca Raton: CRC Press, 2006), p. 789.
2. K. Matsubara and M. Matsuura, in *CRC Handbook of Thermoelectrics*, ed. D.M. Rowe (Boca Raton: CRC Press, 2006), p. 827.
3. H.J. Goldsmid, in *CRC Handbook of Thermoelectrics*, ed. D.M. Rowe (Boca Raton: CRC Press, 1995), p. 37.
4. G. Snyder, in *CRC Handbook of Thermoelectrics*, ed. D.M. Rowe (Boca Raton: CRC Press, 2006), p. 144.
5. W.S. Liu, H. Wang, L. Wang, X.W. Wang, G. Joshi, G. Chen, and Z.F. Ren, *J. Mater. Chem. A* 1, 13093 (2013).
6. J.P. Fleurial, T. Caillat, and A. Borshevsky, *Proceeding of the 13th International Conference on Thermoelectrics* (1994), pp 40–44.
7. B. Poudel, Q. Hao, Y. Ma, Y.C. Lan, A. Minnich, B. Yu, X. Yan, D.Z. Wang, A. Muto, D. Vashaee, X.Y. Chen, J.M. Liu, M.S. Dresselhaus, G. Chen, and Z.F. Ren, *Science* 320, 634 (2008).
8. J.P. Heremans, V. Jovovic, E.S. Toberer, A. Saramat, K. Kurosaki, A. Charoenphakdee, S. Yamanaka, and G.J. Snyder, *Science* 321, 554 (2008).

9. H. Kleinke, *Chem. Mater.* 22, 604 (2010).
10. X. Shi, J. Yang, J.R. Salvador, M.F. Chi, J.Y. Cho, H. Wang, S. Bai, J. Yang, W.Q. Zhang, and L.D. Chen, *J. Am. Chem. Soc.* 133, 7837 (2011).
11. X. Yan, G. Joshi, W.S. Liu, Y.C. Lan, H. Wang, S. Lee, J.W. Simonson, S.J. Poon, T.M. Tritt, G. Chen, and Z.F. Ren, *Nanoletters* 11, 556 (2011).
12. S.J. Poon, D. Wu, S. Zhu, W. Xie, T.M. Tritt, and P.T.R. Venkatasubramanian, *J. Mater. Res.* 26, 2795 (2011).
13. G. Joshi, X. Yan, H.Z. Wang, W.S. Liu, G. Chen, and Z.F. Ren, *Adv. Energy Mater.* 1, 643 (2011).
14. M.I. Fedorov and V.K. Zaitsev, *Mater. Matters* 6, 100 (2011).
15. X. Yan, W.S. Liu, H. Wang, S. Chen, J. Shiomi, K. Esfarjani, H.Z. Wang, D.Z. Wang, G. Chen, and Z.F. Ren, *Energy Environ. Sci.* 5, 7543 (2012).
16. X. Lu, D.T. Morelli, Y. Xia, F. Zhou, V.D. Ozolins, H. Chi, X.Y. Zhou, and C. Uher, *Adv. Energy Mater.* 3, 342 (2013).
17. L.D. Zhao, S.H. Lo, Y. Zhang, H. Sun, G. Tan, C. Uher, C. Wolverton, V.P. Dravid, and M.G. Kanatzidis, *Nature* 508, 373 (2014).
18. L.D. Zhao, G. Tan, S. Hao, J. He, Y. Pei, H. Chi, H. Wang, S. Gong, H. Xu, V.P. Dravid, C. Uher, G.J. Snyder, C. Wolverton, and M.G. Kanatzidis, *Science* 351, 141 (2016).
19. F.J. DiSalvo, *Science* 285, 703 (1999).
20. R.P. Gupta, K. Xiong, J.B. White, K.E. Cho, H.N. Alshareef, and B.E. Gande, *J. Electrochem. Soc.* 157, 666 (2010).
21. P.J. Taylor, J.R. Maddux, G. Meissner, R. Venkatasubramanian, G. Bulman, J. Pierce, R. Gupta, J. Bierschenk, C. Caylor, J. D'Angelo, and Z.F. Ren, *Appl. Phys. Lett.* 103, 043902 (2013).
22. D. Kraemer, J. Sui, K. McEnaney, H. Zhao, Q. Jie, Z.F. Ren, and G. Chen, *Energy Environ. Sci.* 8, 1299 (2015).
23. S. Gahlawat, R. He, S. Chen, L. Wheeler, Z.F. Ren, and K.W. White, *J. Appl. Phys.* 116, 083516 (2014).
24. Y. Zhang, M. Cleary, X.W. Wang, N. Kempf, L. Schoensee, J. Yang, G. Joshi, and L.M. Meda, *Energy Convers. Manag.* 105, 946 (2015).
25. Hi-Z Technology, Inc., *HZ-20 Thermoelectric Module*. [http://www.hi-z.com/uploads/2/3/0/9/23090410/hz-20\\_data\\_sheet.pdf](http://www.hi-z.com/uploads/2/3/0/9/23090410/hz-20_data_sheet.pdf). Accessed 19 May 2016.